Linear-Quadratic-Gaussian with Loop-Transfer-Recovery Methodology for an Unmanned Aircraft

D. Brett Ridgely*
Massachusetts Institute of Technology, Cambridge, Massachusetts
and
Siva S. Banda,†Timothy E. McQuade,‡ and P.J. Lynch‡
Flight Dynamics Laboratory, Wright-Patterson Air Force Base, Ohio

The linear-quadratic-Gaussian with loop-transfer-recovery methodology is considered for flight control design. Several advantages of this method, as well as some precautions that practicing designers should consider during application, have been highlighted. A roll attitude control system is designed for an unmanned aircraft using this methodology. It is demonstrated that this methodology is transparent in addressing such issues as uncertainty descriptions, stability robustness, trade-offs between robustness and available actuator power, bandwith limitations, and prefilter design.

Introduction

In recent years, there has been a growing interest in the synthesis of robust controllers. References 1-4 discuss some of the techniques used to solve this problem. Reference 1 allows stable factor uncertainties and uses a factorization approach to synthesize robust controllers. A time-domain method using a linear-quadratic-Gaussian (LQG) formulation was presented in Ref. 2 to design robust controllers when uncertainties in the state, input, and measurement distribution matrices are present. Uncertainties are expressed in terms of interval matrices in Ref. 3, which develops an iterative synthesis scheme. Quantitative feedback theory is used to shape loop transmissions in Ref. 4, where uncertainties and performance specifications are transformed into templates that are used in conjunction with Nichols charts. While most of these techniques deal with real parameter variations, there has emerged another procedure called robustness recovery (Doyle and Stein[5]) that deals mainly with high-frequency modeling uncertainties. Stein and Athans[6] call this procedure the linear-quadratic-Gaussian with loop-transfer recovery (LQG/LTR) methodology. The purpose of this paper is to examine LQG/LTR to highlight its merits and to note some necessary precautions in applying this procedure to the design of robust controllers.

Recall that linear-quadratic-regulator (LQR) designs have desirable robustness properties with guaranteed gain margins of at least -6dB to ∞ and guaranteed phase margins of at least ± 60 deg. In Ref. 7 Doyle showed that arbitrary LQG designs do not possess the guaranteed robustness properties associated with LQR. To eliminate this difficulty, Doyle and Stein[5] developed an LQG procedure that recovers the desirable robustness properties of LQR. This procedure later came to be known as LQG/LTR.[6] LQG/LTR is an integrated procedure in the sense that it uses both frequency and time-domain concepts. Performance and robustness requirements are specified in the frequency domain, while the majority of the calculations are done in the time domain. Extensive descriptions of this design methodology can be found in several references; see, for example, Refs. 5, 6, 8, and 9. Recently, attempts have been made to extend the concepts of LQG/LTR.[10,11] Applications of the LQG/LTR method can be found in Refs. 12-20.

Design Methodology

In this section, the LQG/LTR design methodology will be summarized briefly. For a detailed discussion, see Refs 5, 8, and 9. A summary of the LQG/LTR procedure, when all uncertainties are reflected at the plant output, will be given here. A dual procedure exists for reflecting the uncertainties at the plant input,[5,8,9]

Consider the LQG block diagram shown in Fig. 1. $G_p(s)$ is the plant transfer matrix. In this paper, we assume that $G_p(s)$ is minimum phase. Stein and Athans in Ref. 6 have suggested two alternate ways of applying this method to non-minimum phase systems.

Typically, we need to augment the given plant with additional dynamics, shown as $G_a(s)$, to effect the loop shapes of the system. For example, $G_a(s)$ may be a bank of integrators to achieve integral action in the system, often desirable for performance. $K_{\mathrm{LQG}}(s)$ is the compensator matrix designed using the LQG/LTR procedure. The overall compensator $K(s)$ includes the augmented dynamics $G_a(s)$ and the compensator matrix $K_{\mathrm{LQG}}(s)$ as shown in Fig. 1. We wish to break the LQG loop of Fig. 1 at the plant output and shape the loop-transfer function $G_p(s)K(s)$ so that the closed-loop system will yield: 1) good command following, 2) good output disturbance rejection and 3) good robustness to modeling errors reflected at the plant output. While the first two requirements are low-frequency performance concerns, the third is a high-frequency requirement. These requirements can be interpreted in the frequency domain using singular values.[21] Figure 2 illustrates the bounds imposed on the minimum and maximum singular values of the loop-transfer matrix to meet these requirements. Typical singular-value plots that meet both the low- and high-frequency constraints are shown in the figure.

We will use $G(s)$ to denote the open-loop *augmented* plant

$$G(s) = G_p(s)G_a(s) \tag{1}$$

Presented as Paper 85-1927 at the AIAA Guidance, Navigation and Control Conference, Snowmass, CO, Aug. 19-21, 1985; received Oct. 15, 1985; revision received April 16, 1986.

*Captain, USAF; Graduate Student, Department of Aeronautics and Astronautics. Member AIAA.
†Aerospace Engineer. Member AIAA.
‡Lieutenant, USAF, Aerospace Engineer. Member AIAA.

and $K_{LQG}(s)$ to denote the compensator designed for the augmented plant $G(s)$. The state space form of the augmented system is

$$\dot{x}(t) = Ax(t) + Bu(t) + \Gamma\xi(t) \tag{2}$$

$$y(t) = Cx(t) + \mu \mathrm{In}(t) \tag{3}$$

The performance index to be minimized is

$$J = E\left\{ \lim_{T\to\infty} \frac{1}{T} \int_o^T (z^T z + \rho u^T u) dt \right\} \tag{4}$$

where

$$z(t) = Hx(t) \tag{5}$$

In Eqs. (2-5), the state vector x is $n\times 1$, the control u is $m\times 1$, the measurement y is $m\times 1$, the response z $m\times 1$, and the process noise vector ξ is $k\times 1$. I is an identity matrix. μ and ρ are scalars where $\rho > 0$. A,B,C,H,Γ, and μI are matrices with appropriate dimensions. The process noise ξ and the measurement noise n are assumed to be zero-mean white-noise processes with Gaussian distributions having constant covariances. The procedure is to design a Kalman filter such that the filter loop will satisfy the requirements shown in Fig. 2 and recover this loop shape asymptotically by tuning the regulator. In Fig. 2, σ_i, $\bar{\sigma}$, and $\underline{\sigma}$ are the ith singular value, maximum singular value, and minimum singular value, respectively, of the filter loop-transfer matrix. (For more on singular values, see Refs. 5, 8, and 9. The following two steps briefly explain this procedure.

Step 1: Filter design

Let T_{KF} indicate the Kalman filter loop-transfer matrix given by

$$T_{KF} = C\phi K_f \tag{6}$$

where $\phi = (sI - A)^{-1}$ and K_f is the filter gain. When $\underline{\sigma}[T_{KF}] \gg 1$, the Kalman equality can be used to show that

$$\sigma_i[T_{KF}] \cong \sigma_i[T_{FOL}] \tag{7}$$

where

$$T_{FOL} = \frac{1}{\sqrt{\mu}} C\phi\Gamma \tag{8}$$

Therefore, one should select Γ and μ in such a way that the maximum and minimum singular values of the right-hand side of Eq. (7) meet the performance and robustness bounds and resemble the desired loop shapes of Fig. 2. Compute Eq. (6) using these values of Γ and μ to approximate the desired loop shapes at low frequency.

Step 2: Regulator design

Let the state weighting Q_c and control weighting R_c be chosen as

$$Q_c = H^T H + q^2 C^T V C \tag{9}$$

$$R_c = \rho I \tag{10}$$

where V is any positive definite symmetric matrix and q is a scalar recovery parameter. For convenience, V can be chosen to be the identity matrix and $\rho = 1$. Let K_c denote the controller gain matrix. The compensator matrix $K_{LQG}(s)$ is given by

$$K_{LQG}(s) = K_c(sI - A + BK_c + K_f C)^{-1} K_f \tag{11}$$

By tuning the regulator state weighting ($q\to\infty$), a sequence of LQG compensators is designed which asymptotically recovers the loop shapes from step 1. This recovery process ensures that the singular values of $G(s)K_{LQG}(s)$ will approach the desired loop shapes. The overall compensator $K(s)$ is given by

$$K(s) = G_a(s)K_{LQG}(s) \tag{12}$$

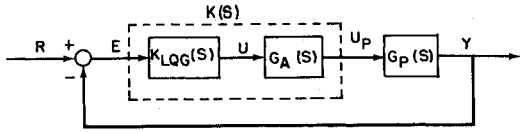

Fig. 1 Block diagram of LQG system.

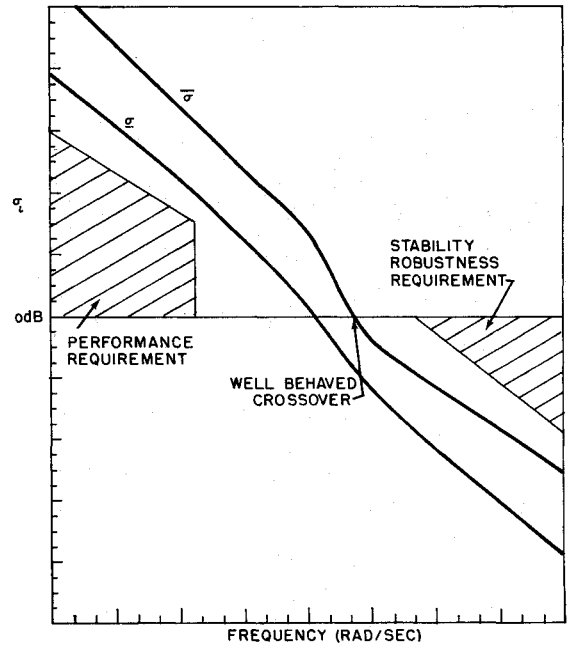

Fig. 2 Desired loop shapes.

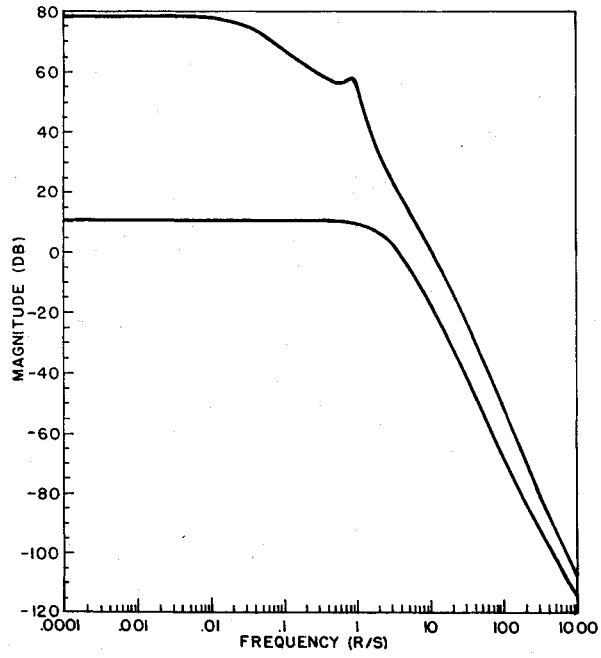

Fig. 3 Singular values of the plant.

Table 1 Numerical data for the example

$$A = \begin{bmatrix} -0.08527 & -0.0001423 & -0.9994 & 0.04142 & 0 & 0.1862 \\ -46.86 & -2.757 & 0.3896 & 0 & -124.3 & 128.6 \\ -0.4248 & -0.06224 & -0.06714 & 0 & -8.792 & -20.46 \\ 0 & -0.06224 & 0.0523 & 0 & 0 & 0 \\ 0 & 0 & 0 & 0 & -20 & 0 \\ 0 & 0 & 0 & 0 & 0 & -20 \end{bmatrix}$$

$$B = \begin{bmatrix} 0 & 0 \\ 0 & 0 \\ 0 & 0 \\ 0 & 0 \\ 20 & 0 \\ 0 & 20 \end{bmatrix} \quad C = \begin{bmatrix} 1 & 0 & 0 & 0 & 0 & 0 \\ 0 & 0 & 0 & 1 & 0 & 0 \end{bmatrix}$$

Table 2 Pole-zero configuration of $C\phi B$

Poles:	
Spiral mode	$-\ 0.036$
Dutch roll (unstable)	$+\ 0.1884 \pm j1.0511$
Roll divergence	$-\ 3.2503$
Elevon actuator	$-\ 20.0$
Rudder actuator	$-\ 20.0$
Zeros:	-158.15

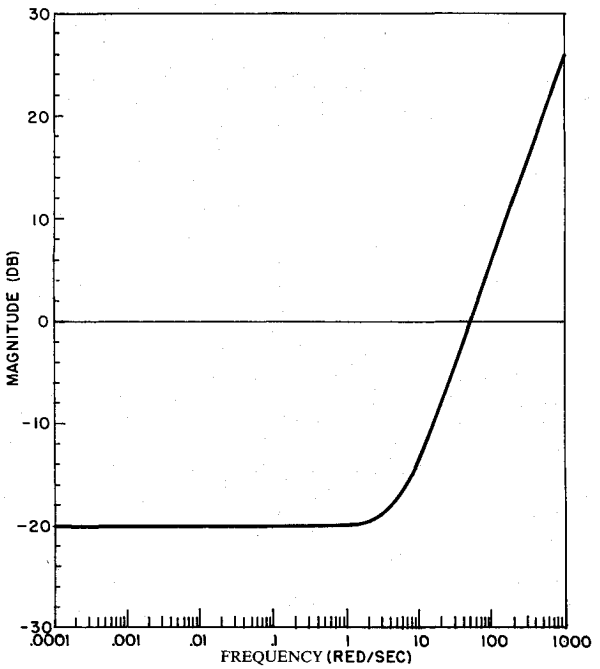

Fig. 4 Uncertainty profile.

It is clear from steps 1 and 2 that the free parameters in the design are the matrix Γ and the scalars μ, ρ, and q.

In this formulation, when the plant is augmented with a bank of integrators, the Kalman filter will estimate these additional states, along the plant states. Simplifying (by designing a reduced-order Kalman filter) or bypassing these additional states in the Kalman filter requires major changes in the formulation of this methodology and are not in the scope

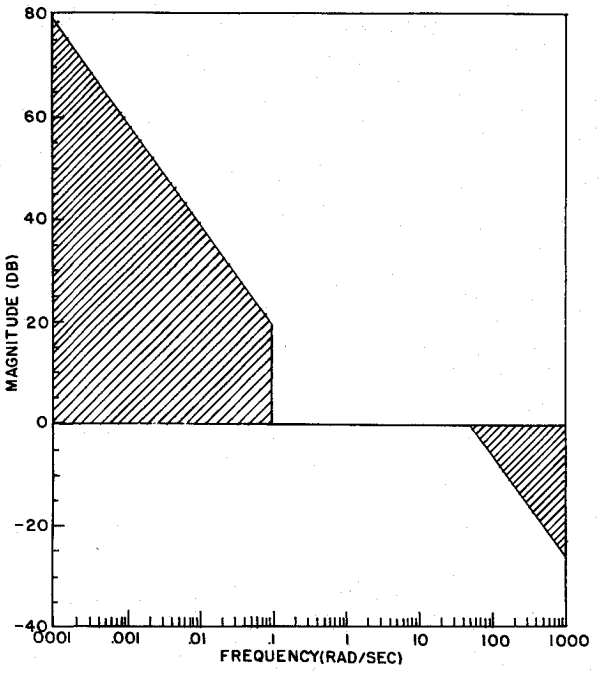

Fig. 5 Performance and stability barriers.

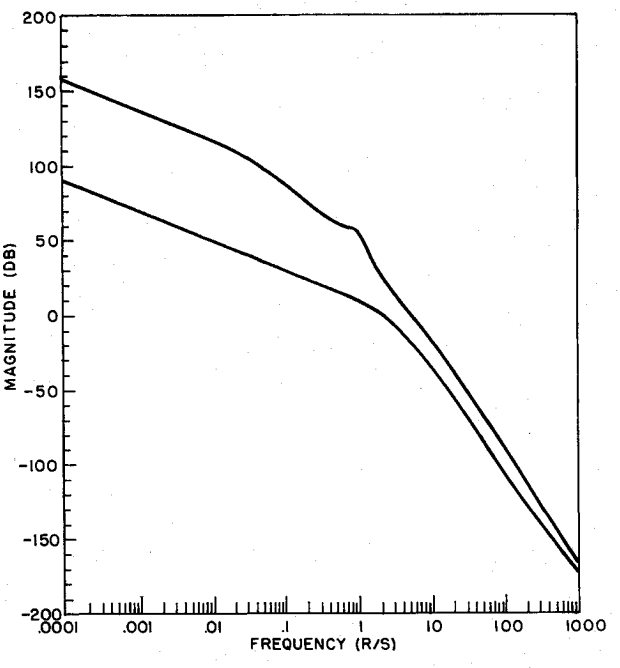

Fig. 6 Singular values of augmented plant.

of this paper. The next section will highlight the merits and some of the concerns in using this methodology.

Remarks on the Use of LQG/LTR

Let us now take a detailed look at this method. First of all, this is an excellent method as long as we know its limitations and do not apply it blindly. The remainder of the discussion in this section should *not* be taken as criticism of the method; rather, it should be taken as a precautionary note. Step 1 uses singular values to measure the magnitude of transfer function matrices in order to extend the classical Single Input Single Output (SISO) loop shaping requirements to Multiple Input Multiple Output (MIMO) systems.[21] The desired loop shape is determined from performance specifications (in the frequency domain), stability

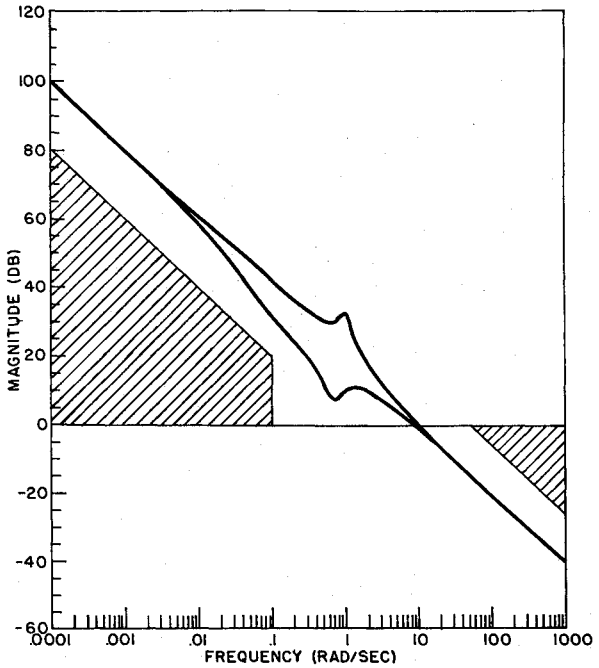

Fig. 7 Singular values of T_{FOL}.

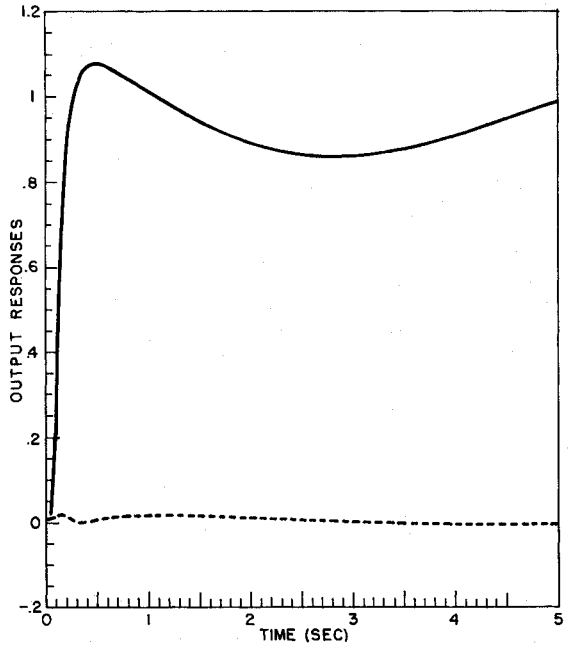

Fig. 8 Time response due to unit step roll command.

robustness bounds based on the uncertainty profile, and the desired system boundaries. The result of step 1 is the matrix T_{KF}, which will be used in step 2. The theoretical proofs used to arrive at step 2 equate loop properties of full-state designs (at either the plant input or output, depending on where uncertainty is reflected) to those of LQG designs. The results show that full-state properties can be "recovered" asymptotically in an almost "mechanical" fashion during step 2. Consequently, the key portion of an LQG/LTR design is judicious use of design freedom available in selecting desired loop shapes. Arriving at the desired loop shapes involves a good deal of engineering judgment. Selection is critical because the filter loop shapes will approximate the desired loops, which will then be recovered during step 2. If the desired loop shapes are bad, the recovered loop shapes will be unsatisfactory, resulting in a poor design. In this case, the desired loop shapes should be altered, and a redesign of the filter and regulator is necessary.

Desired Loop Shapes

Let us consider what is involved in obtaining specific desired loop shapes for a MIMO system. To meet the imposed requirements of good command following and disturbance rejection, high loop gains are required at low frequencies. Additionally, integral action in the loops is normally desirable to obtain zero steady-state error while tracking a constant command. These two general requirements are combined in a scalar function $p(\omega)$. In addition to these low-frequency requirements, uncertainties in modeling impose high-frequency bounds. Errors in sensor dynamics and high-frequency plant modeling are described as an output multiplicative perturbation matrix. The design method uses an estimate of the upper bound $\ell_m(\omega)$ on this perturbation matrix. Analytically obtaining an accurate representation of $\ell_m(\omega)$ is an open question. Estimates of $\ell_m(\omega)$ may be obtained through simulations, which can be expensive in the research phase. Consequently, for the purposes of this study, we have made a rough estimate of uncertainty by assigning a maximum bound consistent with the qualitative statement "uncertainty is high at high frequencies and low elsewhere." The low-frequency barrier of Fig. 2 is given by $p(\omega)/(1-\ell_m(\omega))$, and the high-frequency barrier is given by $1/\ell_m(\omega)$. An additional constraint is that the selected bandwidth of the loop-transfer matrix must be less than the frequency where the uncertainty bound becomes greater than unity. After selecting a practical bandwidth, the loop shapes have to be chosen such that they lie above the low-frequency barrier and below the high-frequency barrier.

Once the desired loop shapes are selected, the matrix Γ and the scalar μ need to be selected so that $\sigma_i[T_{FOL}]$ will produce the desired loop shapes. First of all, it is clear that every element of the matrix Γ needs to be selected. Since $1/\sqrt{\mu}$ is simply a gain factor, it only raises or lowers the singular-value plots, affecting the bandwidth of $\sigma_i[T_{FOL}]$ and the dc gain. After approximating these loop shapes by $\sigma_i T_{KF}]$, one notices that regardless of what $\sigma_i\ T_{FOL}]$ is, $\sigma_i[T_{KF}]$ will always exhibit a 20-db/decade rolloff. This brings an interesting point to our attention. If the $1/\ell_m(\omega)$ plot rolls off with greater than a 20-db/decade slope, then $\sigma_i[T_{KF}]$ inevitably crosses the high-frequency barrier, and one may be tempted to conclude that the final design (after the recovery procedure) will fail the robustness test. This is not true. Step 2 recovers the loop shapes $\sigma_i[T_{KF}]$ by making the regulator fast. Thus, the overall loop-transfer matrix $G(s)K(s)$ will have at least one additional pole-zero excess than that of T_{KF}, resulting in a faster rolloff. Therefore, by proper selection of the recovery parameter q, the intersection of $G(s)K(s)$ and the robustness barrier can be avoided. Notice that, in this case, an upper bound is imposed on q, since as q increases, the additional rolloff is pushed further out in frequency.

Referring again to Fig. 2, the actual bandwidth of $G(s)K_{LQG}(s)$ lies somewhere between the bandwidths of $\underline{\sigma}[GK_{LQG}]$ and $\bar{\sigma}[GK_{LQG}]$. If it is desired to have all the loops behave in the same way, it is necessary to make these loops tight (i.e., get $\underline{\sigma}[GK_{LQG}]$ and $\bar{\sigma}[GK_{LQG}]$ close together at all frequencies). It is possible, using formal loop shaping,[6,9] to pull singular-value plots close together. These tight loops may not always be the best type of loop shapes. If such tight loops are desired, we pay a price in the form of additional states in the system due to the augmentation. This results in a higher-order compensator. A simple technique available to draw the maximum and minimum singular values together is outlined in Ref. 14. This technique will not match the minimum and maximum singular values at all frequencies; rather, it matches them at low and/or high frequencies. However, it may be important to bring these singular values together near the crossover frequency, which this technique does not, in general, allow.

Recovered Loop Shapes

In step 2, the recovery method asymptotically ($q \to \infty$) inverts the plant ($C\phi B$) and replaces it with the full-state design. If the recovery is done using the LQ regulator, then as $q \to \infty$, some of the regulator poles (which are a subset of the closed-loop poles) will approach the zeros of the *plant*. If the plant has zeros either on the imaginary axis or close to it (in the left half-plane), the closed-loop system will display oscillatory behavior. If the plant has a zero in the right half-plane (nonminimum phase plant), the full-state recovery is not possible. The loop-transfer function $G(s)K_{LQG}(s)$ will not converge to the full-state loop-transfer function; rather, it will converge to the solution of H_2-optimization problem.[6] Lightly damped and/or low-frequency open-loop poles may also be undesirable. When a formal loop-shaping procedure (which does not include these poles in the desired loop shape) or certain singular-value matching techniques[14] are used, approximate plant inversion takes place, resulting in zeros close to these lightly damped/low-frequency poles. Therefore, the closed-loop filter poles will be close to their open-loop locations, and since these are a subset of the overall system's closed-loop poles, the system response will be poor. Therefore, it can be seen that lightly damped, low-frequency, open-loop poles, as well as zeros near the imaginary axis or in the right half-plane, present difficulties to direct use of LQG/LTR. This is not to say that LQG/LTR does not work for these cases—only that the designer must be aware of the properties of the system that is being compensated.

Another comment concerns breaking the loop at the output as opposed to breaking at the input. The LQG/LTR procedure requires performance requirements (e.g., command following and disturbance rejection) to be specified at the same location where the uncertainties are represented. Breaking the loop at the output is reasonable because meaningful performance can be specified by requiring the outputs of the plant to follow the commanded inputs and by requiring rejection of disturbances that appear at the output of the plant. Now, consider the case of breaking the loop at the plant input. While requiring input disturbance rejection is reasonable, our command following requirement is still an output specification. That is, we *still* want our outputs to follow our commands, and therefore desire GK to be large at low frequency. Shaping KG (which is what we do for input breaking) to be large at low frequency does *not* guarantee that GK will also be large, since GK and KG do not, in general, commute.

Finally, it should be noted that often it is not possible to satisfy all the control objectives by feedback alone. Open-loop compensation or prefiltering may be necessary to achieve desirable input-output system characteristics from commands to controlled outputs. A formal procedure to design a multivariable prefilter is suggested in Ref. 22. The procedure used there is similar to the formal loop-shaping procedure. It attempts to approximately invert the closed-loop plant and replace it with the desired prefilter dynamics. In this paper, however, a heuristic method is used to design the prefilter. An example will be discussed in the next section.

Design Example

Consider the problem of designing a lateral attitude control system for an unmanned aircraft.[23] The plant is described by the triple (A, B, C) shown in Table 1. The state and control vectors are given by

$$x = [\beta \ \S\phi \ \S\psi \ \phi \ \delta_e \ \delta_r]^T \tag{13}$$

and

$$u = [{}^{\delta}e_c \ {}^{\delta}r_c]^T \tag{14}$$

The states and inputs in Eqs. (13) and (14) are, in order: sideslip, roll rate, yaw rate, roll angle, elevon surface deflection, rudder surface deflection, elevon servo command, and rudder servo command. The nominal Γ matrix will not be specified, except for its dimension, which is (6×2). The strengths of $\xi(t)$ and $n(t)$ are assumed to be unity.

Notice that two changes have been made to the data given in Ref. 23. The first change is that the roll-rate equation includes the effect of yaw rate. This is done to obtain a more realistic model. A second change is that sideslip angle and roll angle are assumed to be measurable quantities. This change is made so that the transmission zeros of $C\phi B$ are located properly in the open left half of the S plane (see discussion in the preceding section). Sideslip angle and roll angle will also be the responses that will be controlled, so that in the response equation (5), $H = C$. A controller will be designed to allow the aircraft to follow a step roll angle command with no (steady-state) change in sideslip.

The poles and zeros fo the open-loop plant $C\phi B$ are shown in Table 2. The singular-value plot of $C\phi B$ is shown in Fig. 3. Notice that the plant has widely separated singular values at low frequency, does not exhibit integral action, and has a natural bandwidth of about 12 rad/s.

Finally, performance and robustness requirements must be established. Mathematically, this translates into defining the scalar functions $p(\omega)$ and $\ell_m(\omega)$. For $p(\omega)$, it is assumed that the loop-transfer function is required to have at least a 20-dB gain at $\omega = 0.1$ rad/s. The system is also required to track command inputs with zero steady-state error, thus requiring integral action. A restriction of 10 rad/s for the maximum crossover frequency of the system is also imposed. For robustness requirements, it is assumed that the model is reasonably accurate (to within 10% of the true plant) up to 2 rad/s, and then the uncertainty grows without bound at the rate of 20 dB/decade. This produces the $\ell_m(\omega)$ curve shown in Fig. 4. It is assumed that this $\ell_m(\omega)$ represents either input or output multiplicative perturbations. These requirements on performance and robustness impose limitations on the loop-transfer function. Barriers for these requirements are shown in Fig. 5.

It should be noted that since the system is square, the design methodology can be carried out by breaking the loop either at the input or at the output. Several controllers were designed for breaking the loop both at the input and at the output of the plant. For brevity, only two designs (both with the loop broken at the output) will be discussed here (see Ref. 9 for other designs).

It is obvious from Figs. 3 and 5 that in order to meet the performance requirements, the plant needs to be augmented with integrators to achieve integral action in both loops. This is done by cascading a bank of integrators in front of the plant. The singular values of the augmented plant are shown in Fig. 6.

Design 1: Select Γ for low- and high-frequency matching.

The matrix Γ is selected such that

$$\sigma_i[T_{FOL}] \cong I/s \tag{15}$$

This is done by choosing Γ as[15]

$$\Gamma = \begin{bmatrix} -(CA^{-1}B)^{-1} \\ C^T(CC^T)^{-1} \end{bmatrix} \tag{16}$$

It should be noted that the matrices A, B, and C in Eq. (16) are for the unaugmented plant. Adjustment of the scalar μ so that the bandwidth of T_{FOL} is close to 10 rad/s produces a value of $\mu = 0.01$. The plot of $\sigma_i(T_{FOL})$ is shown in Fig. 7. Note that all the specifications are met through this selection of Γ. The loops display nearly I/s behavior except for a "rise" and "dip" near 1 rad/s. This can be explained by examining the poles and zeros of T_{FOL} shown in Table 3.

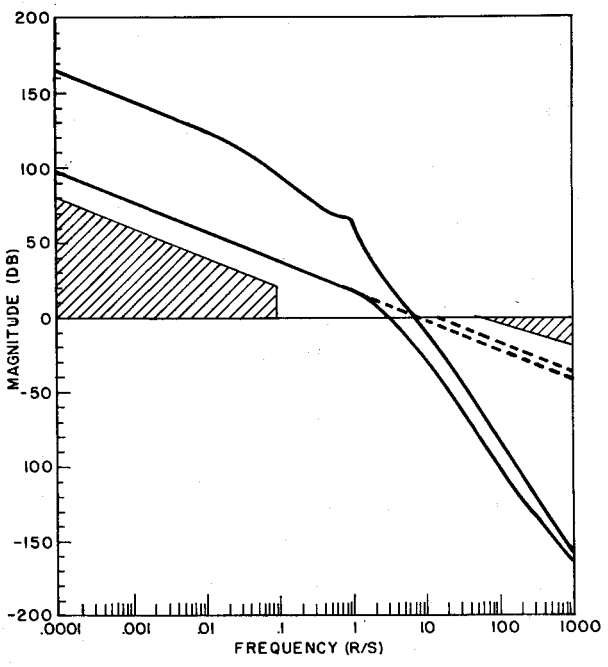

Fig. 9 Singular values of T_{FOL} and T_{KF}.

Table 3 Pole-zero configuration of T_{FOL}

Poles	Zeros
− 0.036	− 0.075
+ 0.1884 ± *j*1.0511	+ 0.168 ± *j*0.737
− 3.2503	− 3.14
−20.0	−19.96
−20.0	−19.99
0.0	
0.0	

Table 4 Zeros of T_{KF}

Zeros:	− 0.074
	− 0.144 ± *j*0.714
	− 3.18
	−20.0
	−20.02

Table 5 Poles of $[A\text{-}K_fC]$

Poles:	− 0.074
	− 0.184 ± *j*0.732
	− 3.05
	−20.0
	−20.08
	−10.02 ± *j*1.41

Obviously, the poles of T_{FOL} are just those of the plant plus those of the augmented integrators. It can be seen that the poles and zeros of T_{FOL} nearly "cancel" each other except for the integrator poles and a mismatch in the complex pole-zero pair. The mismatch in the complex pair is the reason the rise and dip are present in Fig. 7. The rise corresponds to the pole frequency of 1.067 rad/s and the dip to the zero frequency of 0.756 rad/s. The fact that only the integrators effectively remain yields the overall *I/s* behavior of the singular-value plots.

Note that this selection of Γ yields a nonminimum phase T_{FOL}. This occurs because the plant is open-loop unstable and we are trying to invert the plant. Realize that the plant inversion is necessary since we want the singular values to be matched and to look like *I/s*. The Kalman filter can never be nonminimum phase. Therefore, we should expect to see these zeros mirrored to their stable images when we compute T_{KF}.

The gain K_f is calculated using the values of Γ and μ that were just chosen. It was observed that $\sigma_i[T_{KF}]$ are literally identical to $\sigma_i[T_{FOL}]$ and are shown here. Obviously, the poles of T_{KF} are the same as those of T_{FOL}. The zeros of T_{KF} (shown in Table 4) are almost identical to the zeros of T_{FOL} except that the nonminimum phase complex pair in Table 3 is nearly mirrored into the stable half-plane, as expected.

Now the difficulty begins. The next step is to close the loop on the filter and compute the filter poles. Recall that the closed-loop filter is just $C\phi K_f$ with unity feedback around it. The filter poles (poles of $[A-K_fC]$) are given in Table 5. The zeros are invariant under feedback and are therefore the same as those in Table 4.

Recall that the poles shown in Table 5 are a subset of the poles of the overall closed-loop system. Obviously, the complex poles and the pole near the origin are not at all desirable. These two-frequency poles cause a long settling time and the complex pair produces an oscillatory response. However, the close proximity of zeros to these pole locations yield small residuals, which reduce their adverse effects. This near cancellation happens because all the zeros of T_{KF} are very close to the stable images of the plant poles (except the two zeros at infinity). These poles will migrate toward the zeros and therefore will not move significantly (the only poles that move very far are due to the integrators that go toward the zeros at infinity). In general, any time Γ (and/or K_f) is chosen to "invert the plant," the (closed-loop) filter poles will be very close to the stable images of the open-loop poles. If the open-loop poles or their stable images are in undesirable locations (lightly damped and/or low frequency), we should *not* attempt to invert them.

The regulator gain K_c was obtained during the recovery process with $q^2 = 10^5$. The overall compensator was determined from Eqs. (11) and (12). Singular values of the recovered loop-transfer function $G(s)K(s)$ (not shown here) do satisfy the performance and robustness requirements. The time responses of $\beta(t)$ and $\phi(t)$ to a unit step roll command are shown in Fig. 8. While the sideslip response is excellent, the roll response is highly oscillatory, with a corresponding long settling time. Obviously, this design is not acceptable.

From this discussion, it is clear that although the LQG/LTR design methodology was used to design an overall compensator such that the loop-transfer matrix satisfies specified performance and robustness requirements, the time response is oscillatory and undesirable. The fault, however, is not with the LQG/LTR methodology. Rather, it is the fault of the designer who attempted to invert (stable images of) lightly damped and low-frequency poles of the plant in order to come up with an estimate of the matrix, Γ. In the same spirit, this case also shows the need to examine the designs both in the frequency and time domains.

Design 2: Arbitrary Selection of Γ

Looking back to Fig. 6, it can be noticed that $\sigma_i[C\phi B]$ for the augmented system meets our performance and robustness requirements but does not meet the bandwidth requirement. By increasing the gain, the bandwidth requirement can also be met. Therefore, an obvious choice for Γ is to set it equal to B. To achieve the desired bandwidth, $\mu = 0.3$ was chosen. Figure 9 shows the singular values of T_{FOL} and T_{KF} (dashed line is for T_{KF}). As expected, T_{KF} rolls off with only 20 db/decade, and T_{FOL} rolls off much faster. Also, $\sigma_i[T_{KF}]$ and $\sigma[T_{FOL}]$ are identical at low frequencies. The maximum crossover of T_{KF} is slightly above 10 rad/s, but when that loop shape is recovered, the bandwidth of the recovered loop shape should be within the requirements.

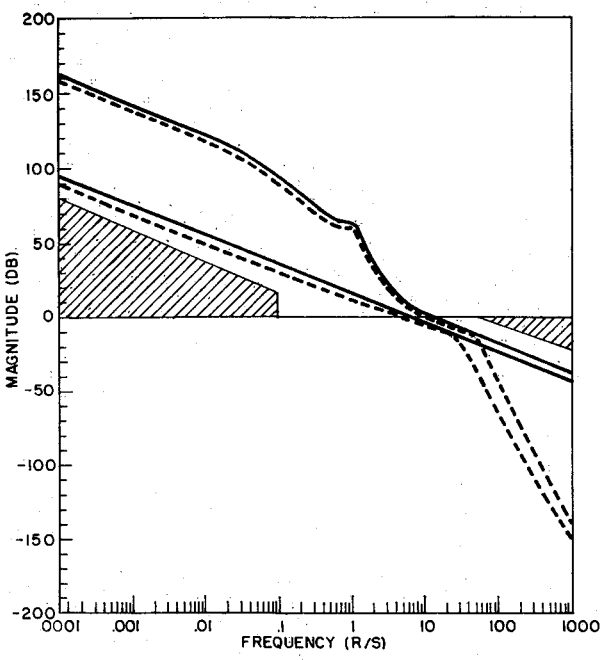

Fig. 10 Singular values of T_{KF} and GK.

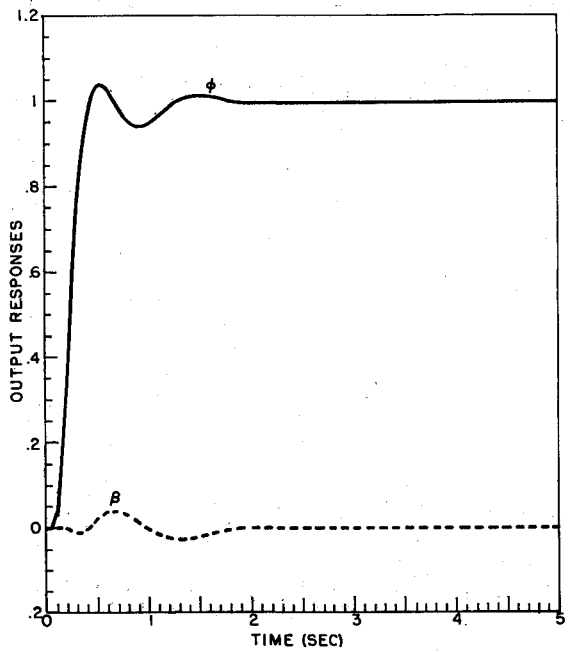

Fig. 11 Time response due to step roll command.

The poles of T_{FOL} and T_{KF} are the same as those shown in Table 3. The zeros of T_{KF} and the poles of the filter are shown in Table 6. The plant (T_{FOL}) has a zero at -158.15. It can be seen that all the filter poles are in "reasonable" locations, so we will proceed with the "recovery." Several choices of q^2 were made ranging from 0 to 10^8. The recovery plots for $q^2 = 10^6$ are shown in Fig. 10 (the dashed line is for GK). The plot of $G(s)K(s)$ meets the specifications. When time responses were examined, they revealed that the design requires high control surface deflection rates and has a large overshoot.

This difficulty is caused by a relatively high maximum bandwidth in the specifications. This difficulty may be remedied by designing a prefilter to slow the response. Through trial and error, a diagonal prefilter transfer matrix with diagonal entries $4/(s+4)$ was chosen. The poll angle and sideslip response to a unit roll command are shown in Fig. 11 and are seen to be almost decoupled. The elevon and rudder surface deflections required for this maneuver are shown in Fig. 12. It can be seen that the maximum surface deflections and rates are reasonable. This was considered to be a good controller design, meeting all the performance specifications and stability robustness requirements.

Table 6 Poles and zeros for design 2

Zeros (T_{KF}):	$-1.92 \pm j1.46$	Filter Poles:	$-1.92 \pm j2.66$
	$-4.07 \pm j3.41$		$-3.31 \pm j5.89$
	-20.0		-3.49
	-20.0		-7.15
			-19.98
			-20.0

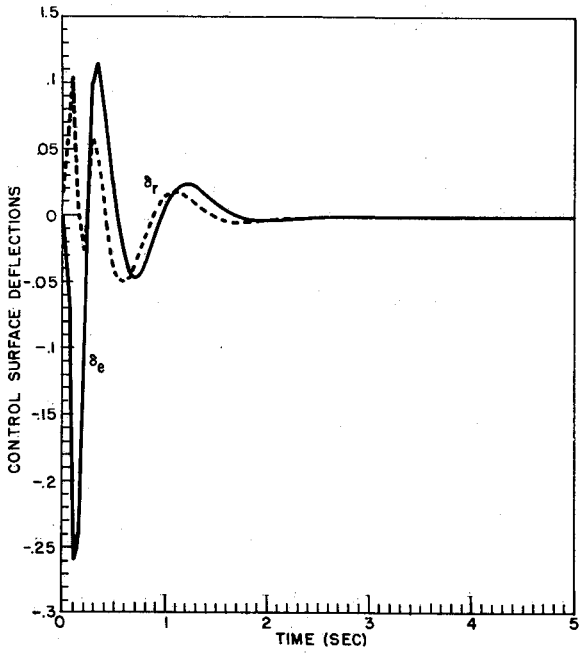

Fig. 12 Required control surface deflections.

Conclusions

The linear-quadratic-Gaussian with loop-transfer recovery is an excellent design methodology that allows the designer to meet low-frequency performance requirements while ensuring closed-loop stability in the face of modeling uncertainties. This technique also makes design tradeoffs reasonably transparent. Like any other design method, it *cannot* be applied blindly. It was pointed out that care should be exercised if the open-loop plant has lightly damped and/or low-frequency poles. Open-loop plant zeros near the imaginary axis are undesirable because some of the closed-loop poles approach these zeros and the closed-loop response may be oscillatory. After finishing the design with this method, it may be necessary to design a prefilter to shape the command inputs to achieve desirable input-output properties of the overall closed-loop system.

References

[1] Vidyasagar, M., "Control System Synthesis: A Factorization Approach," M.I.T. Press, Cambridge, MA, 1985.

[2]Yedavalli, R.K., "Time Domain Control Design for Robust Stability of Linear Regulators," Proceedings of the American Control Conference, Vol. 2, June 1985, pp. 914–919.

[3]Evans, R.J. and Xianya, X., "Robust Regulator Design," *International Journal of Control,* Vol. 41, No. 2, 1985, pp. 461–476.

[4]Horowitz, I.M., "Improved Design Technique for Uncertain Multiple Input-Multiple Output Feedback Systems," *International Journal of Control,* Vol. 36, No. 6, 1982, pp. 977–988.

[5]Doyle, J.C. and Stein, G., "Multivariable Feedback Design Concepts for a Classical/Modern Synthesis," *IEEE Transactions on Automatic Control,* Vol. AC-26, No. 1, Feb. 1981, pp. 4–16.

[6]Stein, G. and Athans, M., "The LQG/LTR Multivariable Control System Design Method," Massachusetts Institute of Technology, Cambridge, May 1984; MIT LIDS-P-1384, May 1984.

[7]Doyle, J.C., "Guaranteed Margins for LQG Regulators," *IEEE Transactions on Automatic Control,* Vol. AC-23, Aug. 1978, pp. 756–757.

[8]Athans, M., *Lecture Notes on Multivariable Control Systems: MIT Subject 6.232,* Massachusetts Institute of Technology, Cambridge, June 1984.

[9]Ridgely, D.B. and Banda, S.S., "Introduction to Robust Multivariable Control," Flight Dynamics Laboratory, Wright-Patterson Air Force Base, OH, AFWAL-TR-85-3102, Feb. 1986.

[10]Madiwale, A.N. and Williams, D.E., "Some Extensions of Loop Transfer Recovery," *Proceedings of the American Control Conference,* Vol. 2, June 1985, pp. 790–795.

[11]Kazerooni, J. and Sheridan, T.B., "An Approach to Loop Transfer Recovery Using Eigenstructure Assignment," *Proceedings of the American Control Conference,* Vol. 2, June 1985, pp. 796–803.

[12]Quinn, W.W., "Multivariable Control of a Forward Swept Wing Aircraft," LIDS-TH-1530, M.S. Thesis, Massachusetts Institute of Technology, Cambridge, Jan. 1986.

[13]Martin, R.J., "Multivariable Control System Design for a Submarine Using Active Roll Control," LIDS-TH-1458, M.S. Thesis, Massachusetts Institute of Technology, Cambridge, May 1985.

[14]Lively, K.A., "Multivariable Control System Design for a Submarine," LIDS-TH-1379, M.S. Thesis, Massachusetts Institute of Technology, Cambridge, May 1984.

[15]Mette, J.A. Jr., "Multivariable Control of a Submarine using the LQG/LTR Methodology," LIDS-TH-1468, M.S. Thesis, Massachusetts Institute of Technology, Cambridge, May 1985.

[16]Haiges, K., "Multivariable Flight Control with Time Scale Separation," LIDS-TH-1381, M.S. Thesis, Massachusetts Institute of Technology, Cambridge, May 1984.

[17]Kapasouris, P., Athans, M., and Spang, H.A. III, "Gain Scheduled Turbofan Engine Using the LQG/LTR Methodology," *Proceedings of the American Control Conference,* Vol. 1, June 1985, pp. 109–118.

[18]Sundararajan, N., Joshi, S.M., and Armstrong, E.S., "Robust Controller Synthesis For a Large Flexible Space Antenna," *Proceedings of the Conference on Decision and Control,* Dec. 1984, pp. 202–208.

[19]Athans, M., Kapasouris, P., Kappos, E., and Spang, H.A. III, "Linear-Quadratic-Gaussian with Loop-Transfer-Recovery Methodology for the F-100 Engine," *Journal of Guidance, Control, and Dynamics,* Vol. 9, Jan.-Feb. 1986, pp. 45–52.

[20]Looze, D., Goodman, G.C., Eterno, J.S., and Athans, M., "Robust Decentralized Control," Flight Dynamics Laboratory, Wright-Patterson Air Force Base, OH, AFWAL-TR-85-3042, Aug. 1985.

[21]Doyle, J.C., "Multivariable Design Techniques Based on Singular Value Generalizations of Classical Control," AGARD Lecture Series 117, *Multivariable Analysis and Design Techniques,* edited by R.E. Pope, Oct. 1981, pp. 1–15.

[22]Lehtomaki, N.A., Stein, G., and Wall, J.E., Jr., "Multivariable Prefilter Design for Command Shaping," *Proceedings of the AIAA Guidance and Control Conference,* Seattle, WA, 1984; AIAA Paper 84–1829, 1984.

[23]Mukhopadhyay, V. and Newsom, J.R., "A Multiloop System Stability Margin Study Using Matrix Singular Values," *Journal of Guidance, Control, and Dynamics,* Sept.-Oct. 1984, pp. 582–587.